

MeV. Similarly, calculations for  $^{25}\text{Mg}$  yrast states excited in the reaction  $^{13}\text{C}(^{16}\text{O}, \alpha)$  show a reduction of a factor of at least 7 at  $E(^{16}\text{O}) = 145$  MeV depending somewhat on the parameters of the Fermi-gas level density.

Thus, a consistent interpretation of the broad structures seen at  $E(^{16}\text{O}) = 145$  MeV can be given by relating them to similar structures observed at much lower bombarding energies where the reaction mechanism is well understood. At lower excitation energies where the high-spin states are well separated ( $\Gamma/D \ll 1$ ) it is necessary to explicitly average over excitation energy to make the broad structures visible. In the statistical model these broad structures arise from angular momentum matching, which creates narrow windows of excitation energy above the yrast level within which a state of spin  $J$  can be excited with significant probability. The spacing of broad structures suggests the  $\Delta J = 1$  sequence plotted in Fig. 3. It must be emphasized that this plot is not unique, however. New data at  $E(^{16}\text{O}) = 145$  MeV (Ref. 5) suggest the possibility that the broad structures at  $E_x(^{24}\text{Mg}) = 45$  and 53.5 MeV may be doublets. This implies that the sequence plotted in Fig. 3 may be incorrect above  $E_x \simeq 45$  MeV. Further high-energy measurement including absolute cross section will be necessary to substantiate the statistical-model description of

these data and determine the shape of the  $^{24}\text{Mg}$  yrast line.

This work was supported in part by the National Science Foundation, by Conselho Nacional de Desenvolvimento Científico e Tecnológico, Brazil, and by the Alfred P. Sloan Foundation.

<sup>1</sup>K. Nagatani, T. Shimoda, D. Tanner, R. Tribble, and T. Yamaya, *Phys. Rev. Lett.* **43**, 1480 (1979).

<sup>2</sup>T. M. Cormier, C. M. Jachcinski, G. M. Berkowitz, P. Braun-Munzinger, P. M. Cormier, M. Gai, and J. W. Harris, *Phys. Rev. Lett.* **40**, 924 (1978).

<sup>3</sup>A. J. Lazzarini, E. R. Cosman, A. Sperduto, S. G. Steadman, W. Thoms, and G. R. Young, *Phys. Rev. Lett.* **40**, 1426 (1978).

<sup>4</sup>W. D. Rae, R. G. Stokstad, B. G. Harvey, A. Dacal, R. Legrain, J. Mahoney, M. J. Murphey, and T. J. M. Symons, *Phys. Rev. Lett.* **45**, 884 (1980).

<sup>5</sup>"Progress in Research," Texas A & M University Cyclotron Institute Report, June 1980 (unpublished).

<sup>6</sup>D. Branford, M. J. Levine, J. Barrette, and S. Kubono, *Phys. Rev. C* **23**, 549 (1981).

<sup>7</sup>R. W. Ollerhead, J. A. Kuehner, R. J. E. Levesque, and E. W. Blackmore, *Can. J. Phys.* **46**, 1381 (1968).

<sup>8</sup>L. K. Fifiield, R. W. Zurmühle, D. P. Balamuth, and J. W. Noé, *Phys. Rev. C* **8**, 2203 (1973).

<sup>9</sup>A. Szanto de Toledo, M. Schrader, E. M. Szanto, G. Rosner, and H. V. Klapdor, *Nucl. Phys.* **A315**, 500 (1979).

<sup>10</sup>Nagatani *et al.*, Ref. 1; N. Takahashi *et al.*, to be published; L. R. Greenwood *et al.*, *Phys. Rev. C* **6**, 2112 (1972).

## Higher-Order Deformations of $^{232}\text{Th}$ and $^{234, 236, 238}\text{U}$

R. M. Ronningen, R. C. Melin,<sup>(a)</sup> J. A. Nolen, Jr., and G. M. Crawley

*Physics Department and Cyclotron Laboratory, Michigan State University, East Lansing, Michigan 48824*

and

C. E. Bemis, Jr.

*Physics Division, Oak Ridge National Laboratory, Oak Ridge, Tennessee 37830*

(Received 10 July 1981)

We have measured the inelastic scattering of 35-MeV protons from  $^{232}\text{Th}$  and from  $^{234, 236, 238}\text{U}$ . Angular distributions were extracted for  $J^\pi = 0^+ - 8^+$  members of the ground-state rotational bands, and were analyzed with use of coupled-channels calculations for scattering from a deformed optical potential. The deformation parameter  $\beta_6$  is positive for  $^{232}\text{Th}$  and  $^{234}\text{U}$ , nearly zero for  $^{236}\text{U}$ , and negative for  $^{238}\text{U}$ . The trends of the deformation parameters and multipole moments are explained qualitatively by a simple model.

PACS numbers: 25.40.Ep, 21.10.Ft, 27.90.+b

The actinide nuclei accessible to scattering experiments are known to be intrinsically deformed and thus their charge and matter (proton and neutron) distributions possess nonzero multipole mo-

ments. The moments best studied experimentally and theoretically are the quadrupole and hexadecapole ("2 $\lambda$  pole," where  $\lambda = 2$  and 4, respectively). Very little information currently exists on

higher-order deformations such as the  $\lambda=6$  (hexacontatetrapole).<sup>1</sup> The present work<sup>2</sup> establishes the systematic variation of the  $\lambda=6$  deformation for the nuclei  $^{232}\text{Th}$  and  $^{234, 236, 238}\text{U}$ .

Apart from the fundamental interest in the nuclear shape the importance of studying deformations of higher order than quadrupole is reflected in the effects they have on nuclear properties. For example, in the heavy transition metals (e.g., W and Os) a stability against oblate ground-state shapes may be attributed to the hexadecapole degree of freedom.<sup>3</sup> Indeed, experimental knowledge of higher-order equilibrium deformations of the actinides can put stringent constraints on theoretical methods for calculating ground-state properties (and thus influences predictions concerning the stability of heavy nuclei). For example, two approaches<sup>4</sup> to the liquid-drop contribution to ground-state energies which give almost the same quadrupole deformations yield substantially different higher-order equilibrium deformations. Furthermore, rotational bands built upon single-particle states<sup>5</sup> and the sizes of gaps in single-particle energies at  $Z=100$  and  $N=152$  depend<sup>3</sup> upon the amount of  $\lambda=6$  deformation.

Empirical evidence for  $\lambda=6$  deformations in actinide nuclei was first shown by Hendrie and co-workers<sup>6</sup> in  $(\alpha, \alpha')$  experiments and by Moss *et al.*<sup>7</sup> in a  $(p, p')$  experiment. But subsequent studies, using Coulomb excitation,<sup>8</sup> and electron<sup>9</sup> and neutron scattering,<sup>10</sup> probed only  $\lambda=2$  and 4 deformations, and thus only confirm theoretical expectations (e.g., Refs. 3 and 11) of how the deformation parameters  $\beta_2$  and  $\beta_4$  vary across a region of deformed nuclei:  $\beta_2$  should attain a maximum value in the middle of the shell and  $\beta_4$  should change sign near that region. For  $\beta_6$ , the early experimental work in the rare-earth region and actinide nuclei used only zero or negative values in the data analysis whereas the calculations by Nilsson *et al.*<sup>11</sup> for the rare-earth and transition-metal nuclei suggest that  $\beta_6$  should change sign twice in the region.

We present here measurements of the  $\lambda=2, 4,$  and 6 deformations of  $^{232}\text{Th}$  and  $^{234, 236, 238}\text{U}$  using proton inelastic scattering at 35 MeV. This is the first systematic study of the  $\lambda=6$  deformations in the actinide region and gives the first evidence for a change in sign of  $\beta_6$  in a deformed region. A 35-MeV proton should be sensitive to the  $\beta_6$  deformation because its wavelength  $\lambda$  is less than 1 fm whereas the  $\beta_6$  deformation induces six surface lobes (see Fig. 1), with about 8 fm between lobes in  $^{238}\text{U}$ .

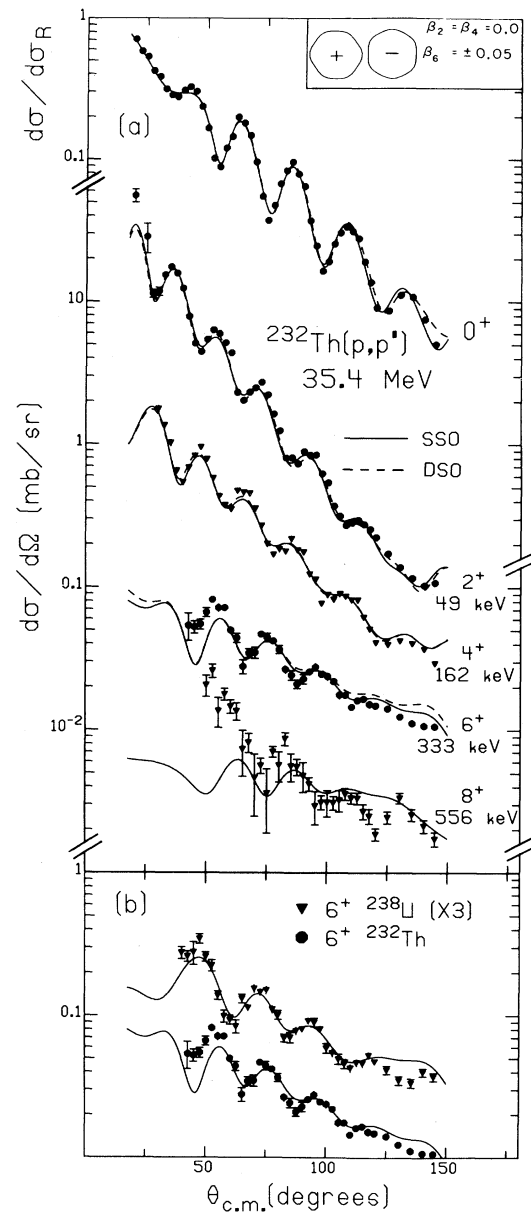


FIG. 1. The inset panel to (a) shows hexacontatetrapole deformations of a sphere. (a) Data and "best fit" coupled-channels calculations for the  $^{232}\text{Th}(p, p')$  reaction, using a full deformed spin-orbit interaction (DSO) and a spherical spin-orbit interaction (SSO). (b) The phase (and magnitude) difference in the  $6^+$  data for  $^{232}\text{Th}$  and  $^{238}\text{U}$ , this due to the different signs of  $\beta_6$ .

The elastic and inelastic scattering reactions using 35-MeV proton beams from the Michigan State University cyclotron were measured in the focal plane of the Enge split-pole spectrometer by using a proportional counter, as previously described.<sup>2</sup> Thorium and uranium tetrafluoride

materials were used to make<sup>2</sup> targets of <sup>232</sup>Th and <sup>238</sup>U. Targets of <sup>234</sup>,<sup>236</sup>U were made<sup>8</sup> in an isotope separator. Angular distributions for elastically and inelastically scattered protons leading to states in the ground-state rotational band with  $J^\pi = 0^+ - 8^+$  in <sup>232</sup>Th are shown in Fig. 1. Our analysis of the data follows closely our previous study<sup>2</sup> where we fit the data using a parametrized deformed optical-model potential (DOMP) to describe the scattering of the protons from the target nucleus modeled by a rigid rotor. In this model inelastic scattering transitions to rotational states are determined by the intrinsic deformations of the nucleus. The deformations are introduced by replacing the radii in the nuclear and Coulomb potentials by  $R(\theta) = r_0 A^{1/3} [1 + \sum_{\lambda} \beta_{\lambda} Y_{\lambda 0}(\theta)]$  where  $\lambda = 2, 4, 6,$  and  $8$ . The deformation parameters  $\beta_{\lambda}$  of the real and imaginary parts of the nuclear potentials were assumed to be equal. In the nuclear potential, a Woods-Saxon radial form was assumed, whereas the Coulomb potential was for a deformed, uniform charge distribution whose moments reproduce those measured by Coulomb excitation.<sup>8</sup> Searches on the standard optical-model parameters  $V$ ,  $W_d$ ,  $V_{so}$ ,  $a_r$ , and  $a_i$  as well as the deformation parameters  $\beta_2$ ,  $\beta_4$ , and  $\beta_6$  were carried out. Both the full deformed (DSO) and spherical (SSO) spin-orbit interactions were used: SSO calculations allowed all levels of the ground band to  $8^+$  to be coupled to  $L = 10$  (with  $\beta_8 = 0$ ) and extensive searches to be made; DSO calculation searches were made by using the values of  $\beta_6$  from the SSO searches; finally, for <sup>232</sup>Th and <sup>238</sup>U, several "one-shot" DSO calculations were performed on a large computer. The results of these approaches were not very different. Table I gives the deformation parameters (for the DSO calculations only). We note that the sign of  $\beta_6$  is positive for <sup>232</sup>Th and <sup>234</sup>U, nearly zero for <sup>236</sup>U, and negative for <sup>238</sup>U.

Figure 1(b) shows the angular distributions for the  $6^+$  states in <sup>232</sup>Th and <sup>238</sup>U. The difference in

the phases of the oscillations is the most striking feature, and, as the calculations show, this helps indicate the difference in the signs of  $\beta_6$  in these two nuclei. Note that the fits to these data are significantly better than in Ref. 2 where  $\beta_6$  deformations were not included.

Deformation parameters and even deformation lengths ( $\beta_{\lambda} R$ ) are model- and reaction-dependent quantities. The multipole moments of an intrinsically deformed charge or matter distribution are more fundamental. With the assumption of axial symmetry, these are

$$q_{\lambda 0} = \int r^{\lambda} Y_{\lambda 0}(\theta) \rho(r, \theta) d^3 r.$$

In Coulomb excitation measurements, for example, with use of the rotational model,

$$B(E\lambda; 0^+ \rightarrow J^\pi = \lambda^+) = q_{\lambda 0}^2.$$

Our analysis follows a procedure suggested by Mackintosh<sup>12</sup> following work by Satchler<sup>13</sup>: To the extent that the DOMP that we use can be derived from folding a realistic nucleon-nucleon interaction with the matter distribution (under the assumption of a density-independent interaction and equal proton and neutron deformations), the moments of our DOMP should be equal to those of the underlying matter distributions. Thus, we calculate

$$q_{\lambda 0} = \frac{Z \int r^{\lambda} V(r, \theta) Y_{\lambda 0}(\theta) d^3 r}{\int V(r, \theta) d^3 r}$$

for  $\lambda = 2, 4,$  and  $6$ , using the parameters in Table I (for the DSO DOMP only; those from the SSO DOMP are the same within statistical uncertainties). These are also given in Table I.

Some time ago, Bertsch proposed<sup>14</sup> a simple picture of how, to first order, intrinsic moments and deformation parameters should vary for nuclei within a major shell [ $q_{\lambda 0}, \beta_{\lambda} \sim \int_{\mu}^1 P_{\lambda}(\mu') d_{\mu}'$  where  $P_{\lambda}(\mu)$  is a Legendre polynomial and  $\mu$  is the cosine of the angle between the symmetry axis and the orbital being filled]. He was thus able to

TABLE I. Deformation parameters  $\beta_{\lambda}$  and multipole moments  $q_{\lambda 0}$  for <sup>232</sup>Th and <sup>234</sup>,<sup>236</sup>,<sup>238</sup>U from coupled-channels calculations using a deformed spin-orbit interaction. The units for  $q_{\lambda 0}$  are  $e \cdot b^{\lambda}$ .

	$\beta_2$	$\beta_4$	$\beta_6$	$q_{20}$	$q_{40}$	$q_{60}$
<sup>232</sup> Th	0.202(2)	0.068(1)	0.009(2)	2.82(4)	0.98(4)	0.30(4)
<sup>234</sup> U	0.214(2)	0.072(2)	0.007(4)	3.12(6)	1.12(7)	0.34(7)
<sup>236</sup> U	0.220(2)	0.063(2)	-0.003(5)	3.17(7)	1.00(7)	0.21(8)
<sup>238</sup> U	0.226(1)	0.052(1)	-0.011(2)	3.25(3)	0.88(3)	0.10(3)

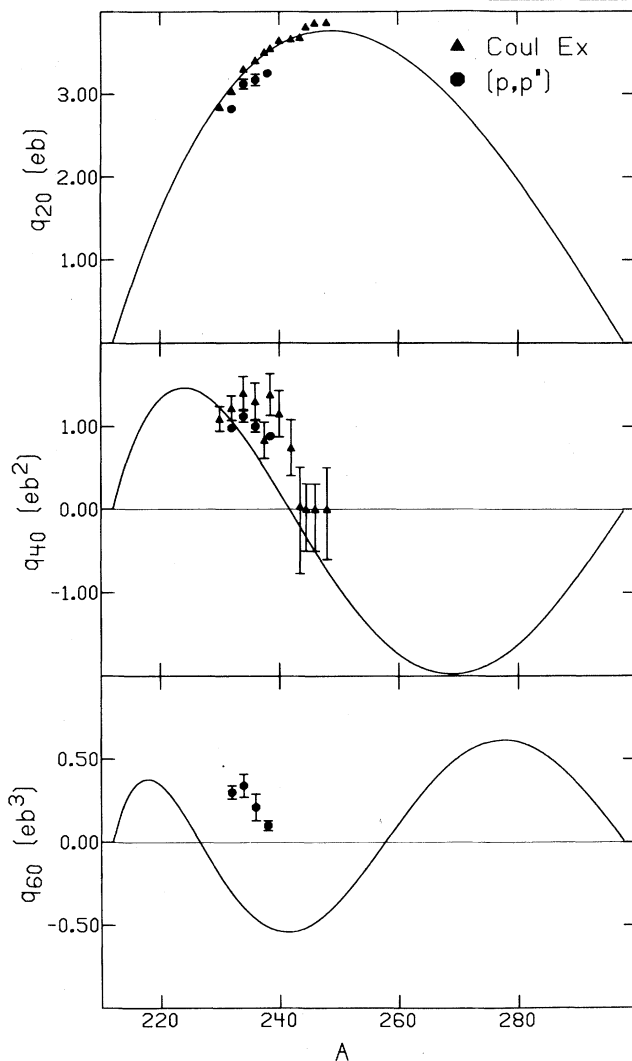


FIG. 2. Values of the quadrupole, hexadecapole, and hexacontatetrapole moments in the actinide region from Coulomb excitation (triangles) (Ref. 8) and the present ( $p, p'$ ) study (circles). The average percentage differences between  $q_{20}$  and  $q_{40}$  values from these two studies (6.7% and 17%, respectively) are consistent with the predictions of Brack *et al.* (Ref. 15) for differences between reduced neutron and proton moments (6.6% for  $q_{20}$  and 22% for  $q_{40}$ ).

explain the existence of positive values of  $\beta_4$  at the beginning of a deformed region and negative values at the end.

Qualitatively, as shown in Fig. 2, the variations of  $q_{20}$  and  $q_{40}$  values across the region are described by Bertsch's model. (The apparent quantitative disagreement in locations of maxima, minima, and crossing points presumably is because the simple picture neglects shell, surface, and Coulomb energy effects.) Quantitatively, the

percentage differences between the values from Coulomb excitation and from our study, which has sensitivity to neutron distributions, are nearly the same as what Brack *et al.*<sup>15</sup> predicted for differences between reduced proton and neutron moments. But, here for the first time in either the rare-earth or the actinide region, a change in sign of  $\beta_6$  is observed, along with an indication that  $q_{60}$  changes sign in the vicinity of  $A \approx 240$ . It is rather remarkable that the simple model of Bertsch predicts this same effect for this order of deformation. The more sophisticated calculations of Nilsson *et al.*<sup>11</sup> also predict the same trend. Further studies of higher-order deformations are needed both in the actinide and rare-earth regions to extend the present results.

This work was partly supported by the National Science Foundation under Grant No. PHY-78-22696. Oak Ridge National Laboratory is operated by the Union Carbide Corporation under Contract No. W7405-eng-26 with the U. S. Department of Energy.

<sup>(a)</sup>Present address: Bell Telephone Laboratories, Murray Hill, N.J. 07974.

<sup>1</sup>C. H. King, private communication. This form is consistent with the form "hexadecapole." "Hexakontatetrapole," also correct, has been used (N. B. "hexakontatetrapole", sic) by R. S. Mackintosh, Rep. Prog. Phys. **40**, 731 (1977).

<sup>2</sup>C. H. King, J. E. Finck, G. M. Crawley, J. A. Nolen, Jr., and R. M. Ronningen, Phys. Rev. C **20**, 2084 (1979). A preliminary report of the present work can be found in R. C. Melin, R. M. Ronningen, J. A. Nolen, Jr., G. M. Crawley, C. H. King, J. E. Fink, and C. E. Bemis, Jr., in Proceedings of the International Conference on Band Structure and Nuclear Dynamics, New Orleans, 1980 (unpublished), Vol. 1, p. 69.

<sup>3</sup>U. Götz, H. C. Pauli, K. Alder, and K. Junker, Nucl. Phys. **A192**, 1 (1972).

<sup>4</sup>P. Möller, S. G. Nilsson, and J. R. Nix, Nucl. Phys. **A229**, 292 (1974).

<sup>5</sup>R. R. Chasman, I. Ahmad, A. M. Friedman, and J. R. Erskine, Rev. Mod. Phys. **49**, 833 (1977).

<sup>6</sup>D. L. Hendrie, B. G. Harvey, J. R. Meriwether, J. Mahoney, J.-C. Faivre, and D. G. Kovar, Phys. Rev. Lett. **30**, 571 (1973); D. L. Hendrie, N. K. Glendenning, B. G. Harvey, O. N. Jarvis, H. H. Duhm, J. Saudinos, and J. Mahoney, Phys. Lett. **26B**, 127 (1968); D. L. Hendrie, Phys. Rev. Lett. **31**, 478 (1973).

<sup>7</sup>J. M. Moss, Y. D. Terrien, R. M. Lombard, C. Brassard, J. M. Loiseaux, and F. Resmini, Phys. Rev. Lett. **26**, 1488 (1971).

<sup>8</sup>C. E. Bemis, Jr., F. K. McGowan, J. L. C. Ford, Jr., W. T. Milner, P. H. Stelson, and R. L. Robinson,

Phys. Rev. C **8**, 1466 (1973).

<sup>9</sup>T. Cooper, W. Bertozzi, J. Heisenberg, S. Kowalski, W. Turchinets, C. Williamson, L. Cardman, S. Fivozinsky, J. Lightbody, Jr., and S. Penner, Phys. Rev. C **13**, 1083 (1976).

<sup>10</sup>Multipole moments from neutron scattering can be found in Ch. Lagrange and J. P. Delaroche, in *Proceedings of an International Conference on Neutron Physics and Nuclear Data for Reactors and Other Applied Purposes*, Harwell, United Kingdom, 1978 (Organization

for Economic Co-operation and Development, Nuclear Energy Agency, Paris, 1978), p. 355.

<sup>11</sup>S. G. Nilsson, C. F. Tsang, A. Sobiczewski, Z. Szymanski, S. Wycech, C. Gustafson, I. L. Lamm, P. Moller, and B. Nilsson, Nucl. Phys. **A131**, 1 (1969).

<sup>12</sup>R. S. Mackintosh, Nucl. Phys. **A266**, 379 (1976).

<sup>13</sup>G. R. Satchler, J. Math. Phys. (N.Y.) **13**, 1118 (1972).

<sup>14</sup>G. F. Bertsch, Phys. Lett. **26B**, 130 (1968).

<sup>15</sup>M. Brack, T. Ledergerber, H. C. Pauli, and A. S. Jensen Nucl. Phys. **A234**, 185 (1974).

## Preequilibrium Emission in the Fusion Reactions in the System $^{14}\text{N} + ^{27}\text{Al}$ at 100 MeV

R. Billerey, C. Cerruti, A. Chevarier, N. Chevarier, B. Cheynis, A. Demeyer,  
and M. N. Namboodiri<sup>(a)</sup>

*Institut de Physique Nucléaire and Institut National de Physique Nucléaire et de Physique des Particules,  
Université Lyon-1 43, F-69621 Villeurbanne, France*

(Received 30 March 1981)

Light-particle emission in the fusion reactions in the system  $^{14}\text{N} + ^{27}\text{Al}$  at 100 MeV has been studied with use of coincident techniques. Comparison of the data with a statistical model accounts for the energy and angular distributions of the products, the particle multiplicities, and the dealignment in the evaporation cascade. However,  $(18 \pm 5)\%$  of the evaporation residue cross section is of nonequilibrium origin and is interpreted in the framework of preequilibrium emission from complex configurations.

PACS numbers: 25.70.Bc

Several studies of heavy-ion reactions have been made recently where light-particle-heavy-fragment coincidence techniques have been employed to explore the reaction mechanism, especially questions regarding the existence of nonequilibrium phenomena. Although the statistical model is very useful in such studies to simulate the equilibrium decay of compound nuclei, detailed application of the model has been made only in a few cases.<sup>1</sup> In this Letter, we report the results of a coincidence study of the light charged particles emitted in the fusionlike reactions of 100-MeV  $^{14}\text{N}$  projectiles with  $^{27}\text{Al}$ . From a comparison of the experimental energy spectra and angular correlations with the predictions of a multistep Monte Carlo statistical-model calculation,<sup>2</sup> we conclude that a significant nonequilibrium component exists in the  $\alpha$  emission leading to evaporation residues (ER). This component is interpreted as preequilibrium emission from complex configurations.

The experiment was performed at the isochronous cyclotron of the Institut des Sciences Nucléaires at Grenoble. Heavy ions produced in the reaction of 100-MeV  $^{14}\text{N}$  with  $^{27}\text{Al}$  were detected with use of a telescope consisting of a gas-ionization  $\Delta E$  detector and a Si  $E$  detector. The H and He particles were detected (in and out of the plane

defined by the heavy-ion detector and the beam axis) with use of a silicon detector telescope consisting of three or four detectors. Both singles and coincident events were tagged and written on magnetic tape, and were analyzed off-line on the HP-21MX computer at the Institut de Physique Nucléaire, Lyon.

Statistical-model calculations were made with use of a multistep Monte Carlo Hauser-Feshbach code which allowed the particle emission probabilities and kinematics to be followed over all the steps in a large number of evaporation cascades.<sup>2</sup> The semiclassical formalism of Ericson and Strutinski<sup>3</sup> was employed to calculate the angular distributions and to follow the direction of the angular momentum of the evaporation residues along the cascade. The parameters chosen were those of Ref. 2 which gave a good fit to the ER mass distributions and energy spectra in light-heavy-ion reactions. In our calculation, the only free parameters were the critical angular momentum for fusion, which was set equal to  $27\hbar$  to reproduce the ER cross section, and the radius parameter for the moment of inertia (1.43 fm) which has been chosen to fit the back-angle light-particle spectra.

We discuss certain aspects of the inclusive ER data first. The magnitude and shape of the an-